


Article

Performance of Multilayer Composite Hollow Membrane in Separation of CO₂ from CH₄ in Mixed Gas Conditions

Shahidah Zakariya ^{1,2}, Yin Fong Yeong ^{1,2,*}, Norwahyu Jusoh ^{1,2} and Lian See Tan ³ 

¹ Chemical Engineering Department, Universiti Teknologi PETRONAS, Seri Iskandar 32610, Perak, Malaysia; shahidah.zakariya@utp.edu.my (S.Z.); norwahyu.jusoh@utp.edu.my (N.J.)

² CO₂ Research Centre (CO₂RES), R&D Building, Universiti Teknologi PETRONAS, Seri Iskandar 32610, Perak, Malaysia

³ Department of Chemical Process Engineering, Malaysia-Japan International Institute of Technology (MJIIT), Universiti Teknologi Malaysia (UTM), Jalan Sultan Yahya Petra, Kuala Lumpur 54100, Malaysia; tan.liansee@utm.my

* Correspondence: yinfong.yeong@utp.edu.my

Abstract: Composite membranes comprising NH₂-MIL-125(Ti)/PEBAX coated on PDMS/PSf were prepared in this work, and their gas separation performance for high CO₂ feed gas was investigated under various operating circumstances, such as pressure and CO₂ concentration, in mixed gas conditions. The functional groups and morphology of the prepared membranes were characterized by Fourier transform infrared spectroscopy (FTIR) and field emission scanning electron microscopy (FESEM). CO₂ concentration and feed gas pressure were demonstrated to have a considerable impact on the CO₂ and CH₄ permeance, as well as the CO₂/CH₄ mixed gas selectivity of the resultant membrane. As CO₂ concentration was raised from 14.5 vol % to 70 vol %, a trade-off between permeance and selectivity was found, as CO₂ permeance increased by 136% and CO₂/CH₄ selectivity reduced by 42.17%. The membrane produced in this work exhibited pressure durability up to 9 bar and adequate gas separation performance at feed gas conditions consisting of high CO₂ content.

Keywords: dip-coating; metal organic frameworks (MOFs); multilayer composite hollow fiber membrane; CO₂/CH₄ mixed gas separation



Citation: Zakariya, S.; Yeong, Y.F.; Jusoh, N.; Tan, L.S. Performance of Multilayer Composite Hollow Membrane in Separation of CO₂ from CH₄ in Mixed Gas Conditions. *Polymers* **2022**, *14*, 1480. <https://doi.org/10.3390/polym14071480>

Academic Editor: Zina Vuluga

Received: 11 February 2022

Accepted: 12 March 2022

Published: 5 April 2022

Publisher's Note: MDPI stays neutral with regard to jurisdictional claims in published maps and institutional affiliations.



Copyright: © 2022 by the authors. Licensee MDPI, Basel, Switzerland. This article is an open access article distributed under the terms and conditions of the Creative Commons Attribution (CC BY) license (<https://creativecommons.org/licenses/by/4.0/>).

1. Introduction

Natural gas is a more desirable power source than coal since it has a lower carbon impact [1,2]. Natural gas usually contains 50% to 90% methane (CH₄); nevertheless, harmful contaminants such as water (H₂O), carbon dioxide (CO₂), hydrogen sulfide (H₂S), nitrogen (N₂), ethane (C₂H₆), propane (C₃H₈), and toluene are often found in unprocessed natural gas [3]. With the presence of H₂O, the acid gases CO₂ and H₂S may damage the processing and transportation equipment; thus, raw natural gas must be treated before use [4,5]. In many petroliferous basins, especially in Southeast Asia, high carbon dioxide levels in reservoirs make exploration challenging. The offshore field in Malay Basin's reservoir usually poses high CO₂ concentrations, making exploration difficult. Some fields contain more than 80% CO₂, making them undesirable development prospects [6].

CO₂ removal is crucial in the natural gas purification process. It causes corrosion in pipelines, lowers the calorific value of natural gas, and raises maintenance and operating costs [7]. For the past few decades, membrane technology has reigned supreme in gas separation processes due to its low cost and ease of processing [8,9]. However, the trade-off between permeability and selectivity limits the gas separation performance of the commercially used polymeric materials [10].

Progress in polymeric materials for gas separation has accelerated dramatically in the past few decades, including polysulfone (PSf), cellulose acetate (CA), polyethersulfone (PES), and the polyimide family [11]. PSf has been widely explored and used for membrane

separation among polymeric materials due to its lower material cost and suitable mechanical strength, thermal stability, chemical stability, and gas permeation [12]. However, the well-known “trade-off” between permeability and selectivity caused by the formation of defects, such as the presence of macrovoids on the fiber surface, has resulted in poor gas selectivity [8,9].

To overcome these limitations, various techniques have been proposed, including polymer blending, ultraviolet-assisted graft polymerization, plasma-induced graft polymerization, incorporation of fillers into polymer membrane matrix, and a caulking technique that involves coating the defective membrane skin with highly permeable polymers [13,14]. Surface coating, which is typically coated on porous membrane supports with a highly permeable gutter layer and a selective layer, is one of the most effective ways to improve membrane performance in gas separation [15].

Dip-coating is a popular technique for producing thin-film composite hollow fiber membranes. Thin-film composite membranes with several layers are being developed for use in gas separation applications to enhance the efficiency of thin-film composite membranes. To cover existing flaws and protect the selective layer from abrasion or harmful chemical assaults, the protective layer is usually applied on top of the selective layer [16]. On the substrate surface, the gutter layer is applied to enhance adhesion between the selected selective layer and substrate. Additionally, the gutter layer may help to reduce mass transport resistance since it is usually constructed of highly permeable materials [17].

The gutter layer acts as a bridge between the hollow fiber substrate and the selective layer, while the ultra-thin selective layer separates the gases [18]. It is typical to utilize the Polydimethylsiloxane (PDMS) coating as a gutter layer to smooth the surface, close the macrovoid, and prevent polymers from penetrating into the porous substrate [15]. However, PDMS coatings suffer from low surface energy that can cause poor interfacial adhesion between the gutter layer and the selective layer [19]. As an alternative, a composite selective layer containing inorganic fillers was incorporated into the membrane matrix to improve gas permeability [15]. Typically, rubbery-type polymers are employed because of their softness and flexibility, as well as their controlled gas penetration characteristics due to their solubility selectivity [20]. Many researchers utilize poly(ethylene oxide) (PEO) among various rubbery materials instead of PDMS since it has been identified as the preferable chemical group that interacts effectively with CO₂ [17,18].

Polyether block amide (PEBAX) is a commercially available copolymer composed of polyamide and PEO that is well suited for use as a selective layer material. The benefits of this polymer include high skin formation ability and solvent resistance [21]. Chen et al. used the dip-coating method to prepare PEBA/PDMS/PAN multilayer composite hollow fiber membranes (HFMs) for flue gas treatment. Coating parameters such as polymer content and coating duration were studied, and they found that CO₂ permeance of the composite membranes was improved [20].

On the other hand, over the years, many efforts have been undertaken to develop mixed matrix membranes (MMMs) for gas separation in order to overcome the limitations of polymeric materials. Lately, an MMM consisting of a new type of inorganic filler, metal organic frameworks (MOF), has been widely reported. This type of filler exhibits excellent interaction with polymers owing to its organic linkers and open metal sites [22]. One of the MOF species that shows high porosity is functionalized titanium, also known as NH₂-MIL-125(Ti). In a recent work, Nadia Hartini et al. (2020) incorporated NH₂-MIL-125(Ti) into a 6FDA-durene polymer matrix for CO₂/CH₄ separation. Membranes loaded with 7.0 wt.% of filler showed the highest CO₂ permeability and CO₂/CH₄ selectivity, surpassing the 2008 Robeson upper bound [23]. Similarly, Waqas Anjum et al. found that although employing both MIL-125 and NH₂-MIL-125(Ti) fillers enhances overall separation performance, the NH₂-functionalized filler is recommended since it leads to better selectivity and permeability [24].

In our previous work, we investigated single gas performance of a series of composite membranes containing different compositions of NH₂-MIL-125(Ti) in PEBAX, coated on

a PSf hollow fiber support layer [25]. Enhancement of CO₂ and CH₄ gas permeance was discovered for composite membranes when compared to the PSf membranes coated only with PDMS or PEBAX solutions. Furthermore, the largest increment in CO₂/CH₄ ideal selectivity was found for a composite membrane loaded with 10% of NH₂-MIL-125(Ti) filler [25]. The key reasons for the improvement in CO₂ removal from CH₄ are the high porosity and strong CO₂ affinity of NH₂-MIL-125(Ti) filler [25].

Currently, most of the research on membrane development is concentrated on single gas permeation and draws conclusions about membrane performance based on these data. This technique may cause inaccurate results owing to the lack of impurities and multicomponent gas effects, which greatly degrade pure gas performance [26].

Significant research has been conducted throughout the past few decades, with an emphasis on the modification of various polymeric precursors in the formation of hollow fiber membranes and evaluation of the resultant fibers in single gas permeation. In contrast, relatively few literature works concentrate on binary gas separation [27]. Hence, in this work, we further explore the performance of our previously developed composite hollow fiber membrane in CO₂/CH₄ separation in mixed gas conditions at various operating conditions such as CO₂ feed concentration and pressure. Although in real natural gas purification processing, other impurities are present in the feed stream, the performance of the membrane in CO₂ and CH₄ binary gas mixture separation still could serve as the initial performance indicator prior to upscaling the membrane in real gas separation conditions [28].

2. Materials and Methods

2.1. Chemicals and Materials

Polysulfone, Mw 35,000 supplied from Sigma-Aldrich (St. Louis, MO, USA), was utilized as the polymer matrix phase for the creation of the hollow fiber membrane substrate. N,N-dimethylacetamide (DMAc), ethanol, and tetrahydrofuran (THF) were supplied by Merck and used as received. Polydimethylsiloxane (PDMS) coating layer was supplied by Sigma-Aldrich (St. Louis, MO, USA). Hexane supplied by Merck (Darmstadt, Germany) was utilized as the solvent in the preparation of PDMS coating solutions. Commercial PEBAX MH-1657 polymer was purchased from Arkema Group (Colombes, France). Previously self-synthesized NH₂-MIL-125(Ti) particles were used as fillers [23].

2.2. Fabrication of PSf Hollow Fiber Substrates

The formula for preparing the dope solution is described in detail in our previous work [25]. With the dry/wet spinning process, PSf hollow fiber was spun using a spinneret with dimensions of OD/ID of 0.80 mm/0.4 mm at an air gap distance of 3.0 cm, while the take-up speed was maintained at 5.0 rpm. Then, fibers were immersed in water to remove the solvent residue for three days. Wetted fibers were then washed three times with methanol and n-hexane for 30 min each time. The solvent-exchanged fibers were then dried at room temperature before being subjected to characterization and gas permeation experiments [29].

2.3. Preparation of Gutter Layer and Selective Layer

The coating solution of the gutter layer was prepared by stirring 3 wt.% PDMS in n-hexane. The coating solution of the selective layer was prepared by dissolving PEBAX pellets in a 70/30 ethanol/water solvent mixture at a concentration of 2%. The mixture was agitated under reflux at 85 °C for approximately 2 h until it was fully dissolved, and then a 5–20 wt.% loading of NH₂-MIL-125(Ti) particles synthesized in our previous work (surface area of 1205.9 m² g⁻¹ and pore volume of 0.53 cm³ g⁻¹) [23] was added to the solution. Prior to coating, the NH₂-MIL-125(Ti)/PEBAX suspension was alternately stirred and sonicated for 30 min to ensure complete dispersion of particles in the solution. Subsequently, this solution was stirred and sonicated again to remove any bubbles formed prior to coating. The hollow fiber membranes were first dip-coated for 10 min with PDMS solution as a

gutter layer. Then, the coated hollow fibers were dried for 24 h before being coated with NH₂-MIL-125(Ti)/PEBAX solution. Finally, the composite hollow fibers were cured at room temperature for 48 h before proceeding to gas separation testing. The membranes developed in our previous work [25] and used in this study are shown in Table 1.

Table 1. Membranes prepared in our previous work [25] used in this study.

Code	Multilayer Composite Membranes	Filler Loading (%)
C	PSf/PDMS	0
C ₀	PSf/PDMS/PEBAX	0
C ₅	PSf/PDMS/PEBAX-NH ₂ -MIL-125(Ti)-5wt.%	5
C ₁₀	PSf/PDMS/PEBAX-NH ₂ -MIL-125(Ti)-10wt.%	10
C ₁₅	PSf/PDMS/PEBAX-NH ₂ -MIL-125(Ti)-15wt.%	15
C ₂₀	PSf/PDMS/PEBAX-NH ₂ -MIL-125(Ti)-20wt.%	20

2.4. Characterization of Hollow Fiber Membranes

The crystallinity of all composite membranes was examined by using an X-ray diffractometer (X'Pert3 Powder, Panalytical, Malvern, UK) with Cu K α radiation at ambient temperature. The surface of each hollow fiber sample was irradiated with X-rays and the intensities and scattering angles of the X-rays that leave the samples were measured from 2 θ values of 5° to 35°. In addition, attenuated total reflectance (ATR)-FTIR was used to acquire infrared spectra of the resulting membranes. A total of 50 scans with wavenumbers ranging from 650 to 4000 cm⁻¹ were used to obtain the spectrum of the outer surface of each hollow fiber membrane with a sample size of 1 cm. The morphology of hollow fiber membranes was examined by field emission scanning electron microscopy (FESEM) using a Zeiss Supra 55VP (Jena, Germany). The membrane surface was analyzed for elemental composition using a dispersive X-ray spectrometer (EDS), Bruker Quantax 70 (Berlin, Germany), to confirm the presence of Ti in the NH₂-MIL-125(Ti) particle in the coating layer.

2.5. CO₂/CH₄ Binary Gas Separation Testing

The module was produced by assembling a few 9 cm long fibers prior to the mixed gas permeation test, as illustrated in Figure 1. Both sides of the module were sealed using a 5 min high-performance epoxy glue that was then allowed to dry for 24 h. The module was then placed in a stainless steel pressure chamber for the gas separation test. The binary gas permeability of the resulting membrane was tested from 1 to 9 bar using CO₂/CH₄ binary mixtures containing 14.5 vol %, 42.5 vol %, and 70.0 vol % of CO₂. Gas chromatography (Perkin Elmer, model GCNARL9680, Waltham, MA, USA) equipped with a thermal conductivity detector (TCD) was used to evaluate the gas compositions of feed, retentate, and permeate gas streams. The full experimental and set-up methods have been published elsewhere [30]. The permeability of each gas was calculated by using Equations (1) and (2), which are as follows [31]:

$$P_{\text{CO}_2} = \frac{V_p y_{\text{CO}_2} t}{A_m (P_h x_{\text{CO}_2} - P_l y_{\text{CO}_2})} \quad (1)$$

$$P_{\text{CH}_4} = \frac{V_p y_{\text{CH}_4} t}{A_m (P_h x_{\text{CH}_4} - P_l y_{\text{CH}_4})} \quad (2)$$

where P_{CO_2} , V_p , A_m , P_h , P_l , x , and y are CO₂ permeability (GPU) in the gas mixture, permeate flow rate (cm³(STP)/s), membrane area (cm²), feed pressure (bar), permeate pressure (bar), and the mole fractions of the component in the feed and permeate streams, respectively. The same equations were used to determine the CH₄ permeability in the gas mixture.

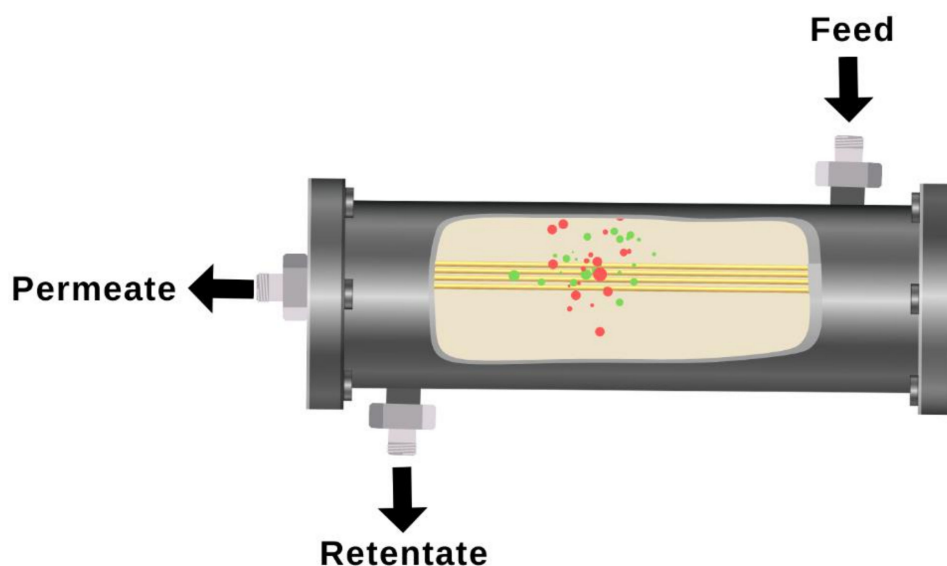


Figure 1. Schematic diagram of the gas permeation test module.

The CO_2/CH_4 mixed gas selectivity was calculated using Equation (3) as follows [32]:

$$\alpha_{\text{CO}_2/\text{CH}_4} = \frac{y_{\text{CO}_2}y_{\text{CH}_4}}{x_{\text{CO}_2}x_{\text{CH}_4}} \quad (3)$$

3. Results and Discussion

3.1. X-ray Diffraction (XRD)

The X-ray diffraction patterns of the resulting membranes are shown in Figure 2. Normally, a polymer sample with an amorphous region exhibits a wide peak intensity [33]. From the results obtained, the XRD pattern for almost all hollow fiber membranes showed a wide band between 15° and 20° . By embedding the particles in the polymer matrix, the membranes became more amorphous, and this result is consistent with the previous results described by Ghasemi et al. [34]. Moreover, the membranes' broad peaks were attributed to the compatibility and full homogeneity of membrane components [35]. Following the integration of the MOFs, the peak locations remained unchanged, demonstrating that there were no changes in the d-spacing of the polymer [27].

3.2. Fourier Transform Infrared Spectroscopy (FTIR)

Figure 3 shows the FTIR spectra of PSf hollow fiber membranes coated with PDMS, PEBAX, and $\text{NH}_2\text{-MIL-125(Ti)/PEBAX}$ containing 5, 10, 15, and 20 wt.% $\text{NH}_2\text{-MIL-125(Ti)}$ particles. The FTIR spectrum of $\text{NH}_2\text{-MIL-125(Ti)}$ shows a broad peak between 3400 and 3700 cm^{-1} , ascribed to $-\text{NH}_2$'s stretching vibration [36]. Peaks between 1658 and 1253 cm^{-1} shown by $\text{NH}_2\text{-MIL-125(Ti)}$ fillers correspond to carboxylic acid functional groups within the MOF structure [37]. Meanwhile, asymmetric stretching vibration bands at 1654 cm^{-1} ($\text{C}=\text{O}$) and symmetric stretching vibration bands at 1253 cm^{-1} ($\text{C}-\text{O}$) observed in the spectrum are attributed to the presence of carbonyl groups in the filler [38]. Peaks between 500 and 800 cm^{-1} are attributed to the O-Ti-O vibration [39]. These remarkable peaks demonstrate the successful synthesis of $\text{NH}_2\text{-MIL-125(Ti)}$. On the other hand, a band at 793 cm^{-1} shown in the FTIR spectrum of PDMS/PSf membrane (C) corresponds to the stretching vibration of $\text{Si}-\text{O}$ bonds. The presence of this band in the FTIR spectrum indicates the presence of PDMS sub-chains in the membrane [40]. Additionally, peaks at 2966 , 1102 , and 1014 cm^{-1} shown in the PDMS/PSf (C) spectrum correspond to the C-H stretching vibrations of Si-CH_3 and Si-O-Si [41].

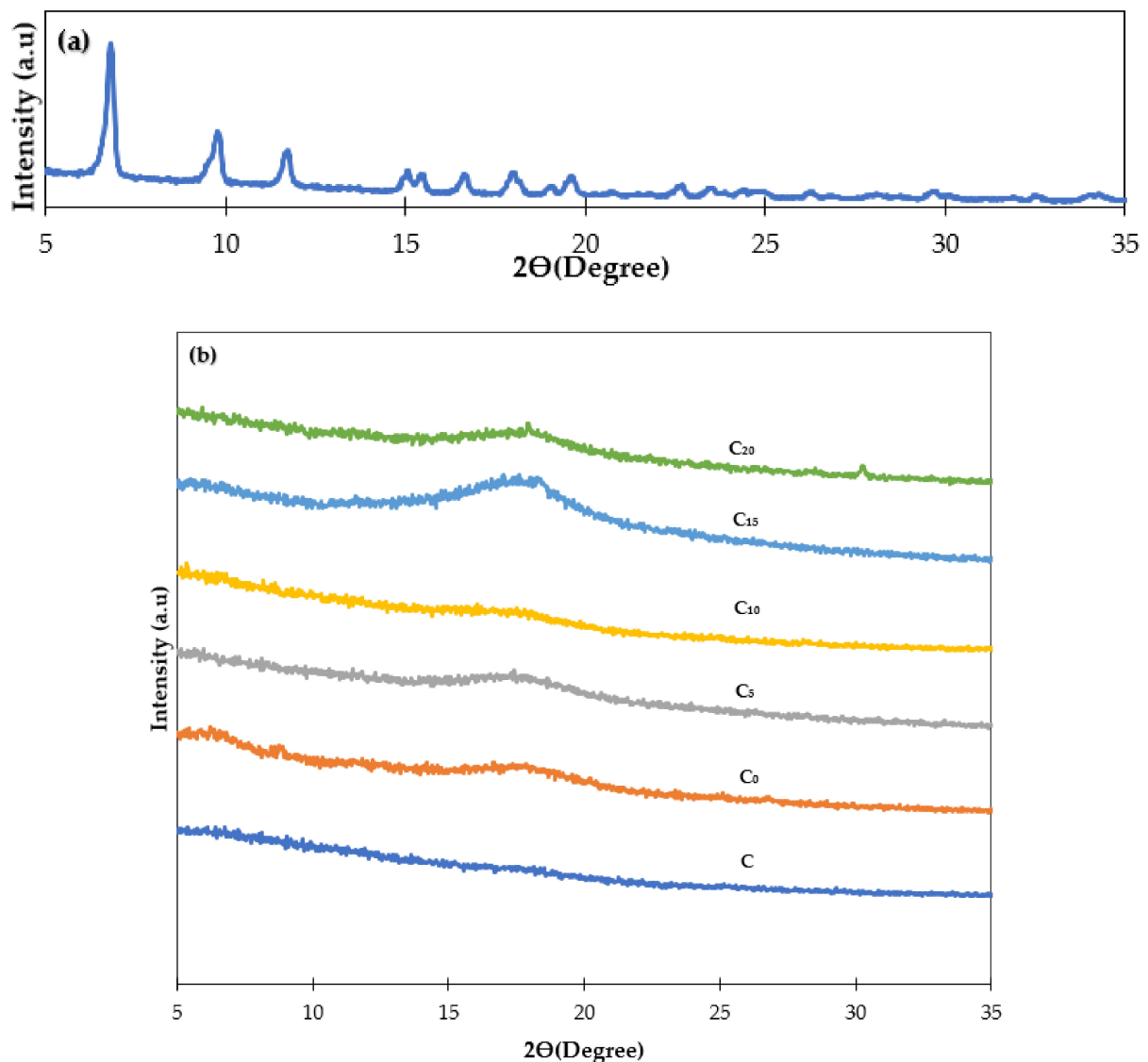


Figure 2. XRD patterns of (a) NH₂-MIL-125(Ti) and (b) composite membranes.

For the PEBAX/PDMS/PSf (C₀) membrane, the distinct peak at around 1238 cm⁻¹ is attributed to the stretching vibration of the C–O–C group within the PEO segment [42]. Furthermore, the membrane exhibits relatively sharp peaks at 3301, 1488, and 1641 cm⁻¹. These peaks are attributed to the hard polyamide segment's –N–H–, H–N–C=O, and O–C=O groups [42]. Referring to Figure 3, membranes C₅–C₂₀ exhibit minor bands from 3400 to 3700 cm⁻¹, corresponding to the –NH₂ stretching vibration from the particles. Considering this, the bands associated with the PEBAX selective layer are stronger, indicating that the PDMS bands detected might be caused by the PEBAX layer.

It can be seen from Figure 3 that membranes C₀–C₂₀ exhibit similar FTIR spectra. However, in comparison with the C₀ membrane, the reduced peak at 1253 cm⁻¹ in the FTIR spectrum of the membrane C₁₀ indicates the interaction of PEBAX and NH₂-MIL-125(Ti). This observation shows that the NH₂-MIL-125(Ti) particles on the surface of fibers disturbed the chain of PEBAX. Additionally, no new peaks were found in the FTIR spectra of composite membranes (C₅–C₂₀), indicating that the NH₂-MIL-125(Ti) and PEBAX were physically blended [43].

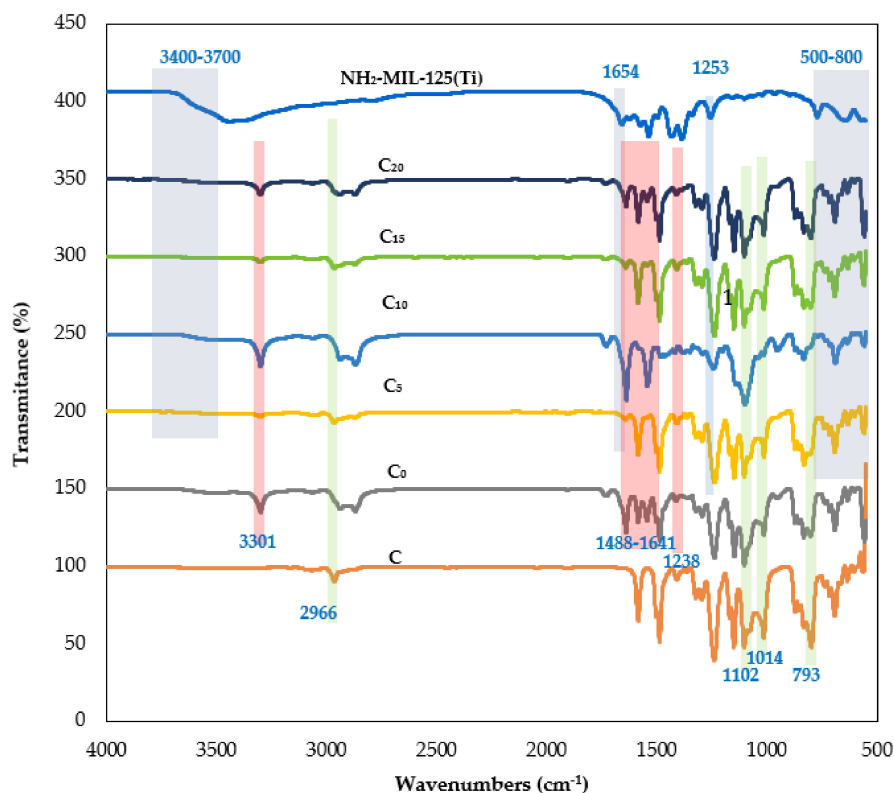


Figure 3. FTIR spectra of fillers and composite hollow fiber membranes.

3.3. Field Emission Scanning Electron Microscopy (FESEM)

Figure 4 shows the FESEM images of PSf/PDMS membrane (C) at the outer surface. The outer surface of the membrane after PDMS coating became denser and smoother. This may help eliminate the solution intrusion during the subsequent coating of the selective layer containing $\text{NH}_2\text{-MIL-125(Ti)}$ in PEBAX.

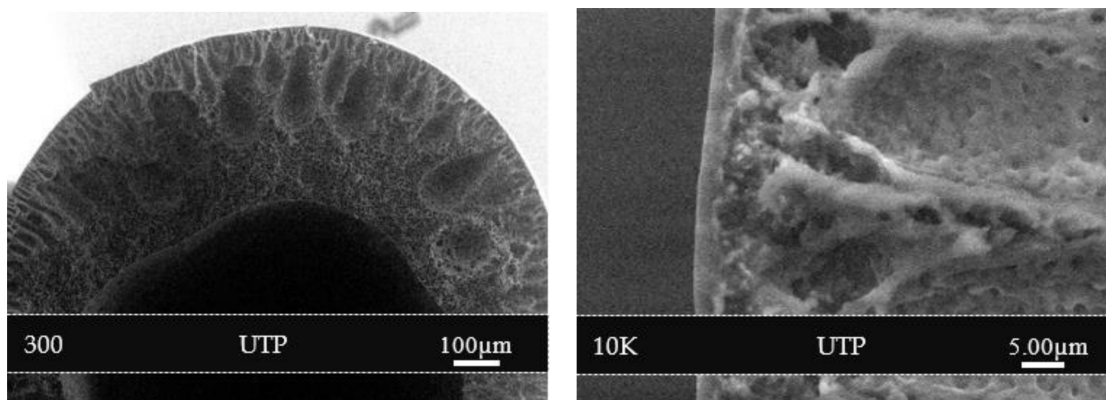


Figure 4. Cross-section morphology of PSf/PDMS membrane (C) at 300 and 10 K magnifications.

The outer skin, which is composed of a PEBAX/ $\text{NH}_2\text{-MIL-125(Ti)}$ selective layer at various filler loadings, is responsible for gas separation, whereas the porous sublayer beneath offers both mechanical support and separation [9]. FESEM images of the PSf hollow fiber coated with PDMS as the first layer and $\text{NH}_2\text{-MIL-125(Ti)}$ /PEBAX as a subsequent layer are shown in Figure 5. From Figure 5, it can be seen that a modest particle dispersion with the same thickness was found for all membranes (Figure 5a–c), where the concave surface is visible and smaller particles were most likely present in the coating dispersion, leading them to adhere to the membrane surface. This is owing to the flexibility of the PEBAX chains, which enables superior contact and adhesion with the $\text{NH}_2\text{-MIL-125(Ti)}$

particle [44]. Figure 5d shows a slight reduction in the thickness of the membrane loaded with 20% $\text{NH}_2\text{-MIL-125(Ti)}$. Ultimately, all the images demonstrate that the PEBAX coating layer provides a conducive environment for the adhesion of $\text{NH}_2\text{-MIL-125(Ti)}$ particles to the membrane surface. In an earlier work, our EDX mapping analysis was performed on the membrane surface to determine the distribution of $\text{NH}_2\text{-MIL-125(Ti)}$ particles in the outer coating layer [25]. The existence of $\text{NH}_2\text{-MIL-125(Ti)}$ on the membrane surface was confirmed by scanning the elements of titanium, the major component of $\text{NH}_2\text{-MIL-125(Ti)}$. Certainly, the dispersion of titanium increased with higher particle loadings.

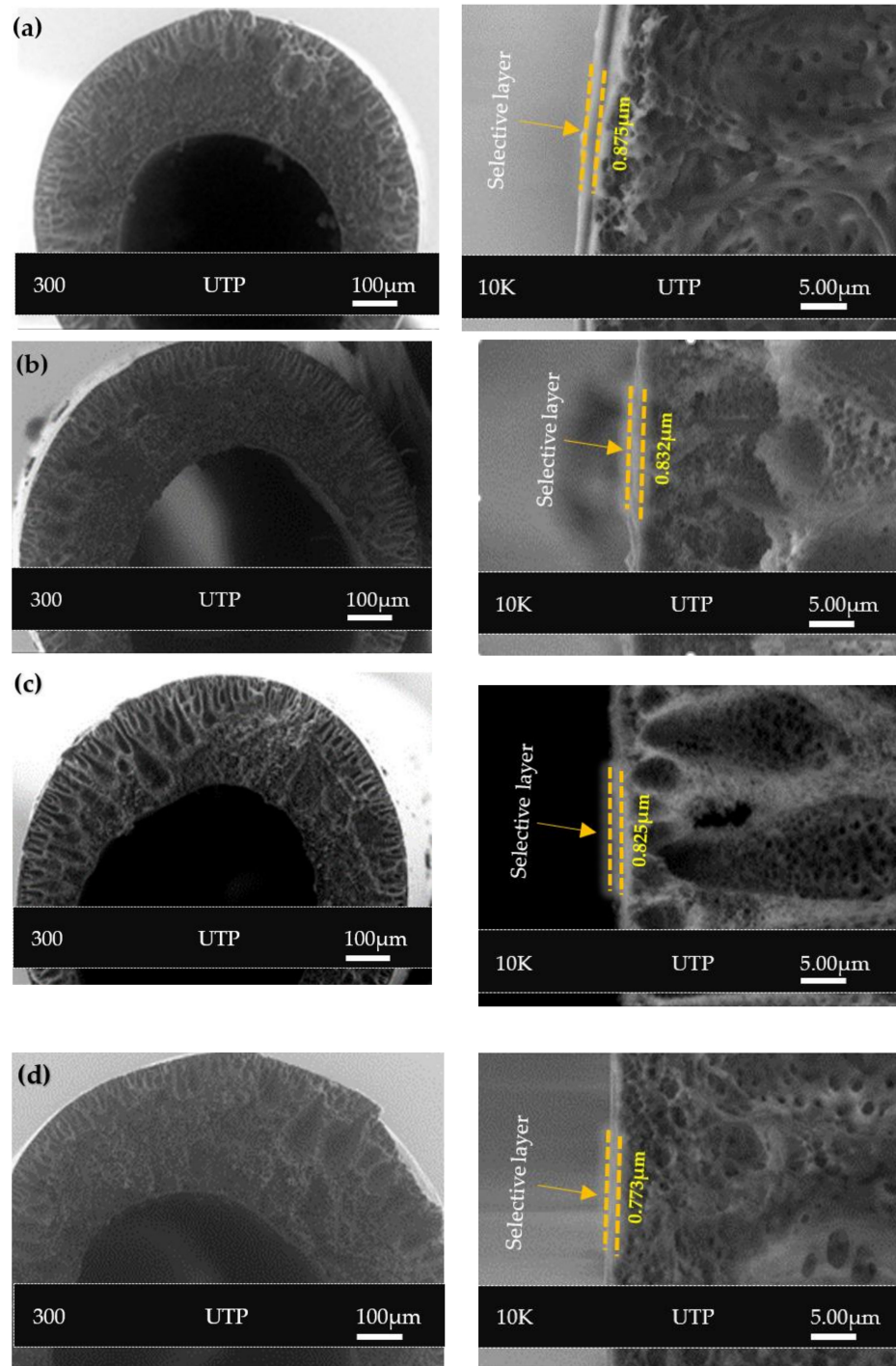


Figure 5. Cross-section morphology of composite hollow fiber membranes at 300 and 10 K magnifications (a) C_5 , (b) C_{10} , (c) C_{15} , and (d) C_{20} .

3.4. CO₂/CH₄ Mixed Gas Separation Performance

3.4.1. Effect of CO₂ Concentration in Feed Stream

Our previous study found that the best single gas permeation performance was exhibited by a composite membrane loaded with 10 wt.% filler (C₁₀) [25]. In the present work, we further explore the performance of this membrane in CO₂/CH₄ separation in mixed gas conditions. Figure 6 shows the effect of CO₂ feed composition on CO₂ and CH₄ permeances as well as the selectivity in mixed gas separation evaluated at 25 °C for the C₁₀ membrane. The CO₂ concentrations ranged from 14.5 vol % to 70 vol % at a feed pressure of 5 bar. CO₂ is well known as a plasticizer for polymeric membranes. The higher the CO₂ content in the membrane, the greater the polymer free volume and segmental mobility, resulting in a decrease in membrane selectivity [45].

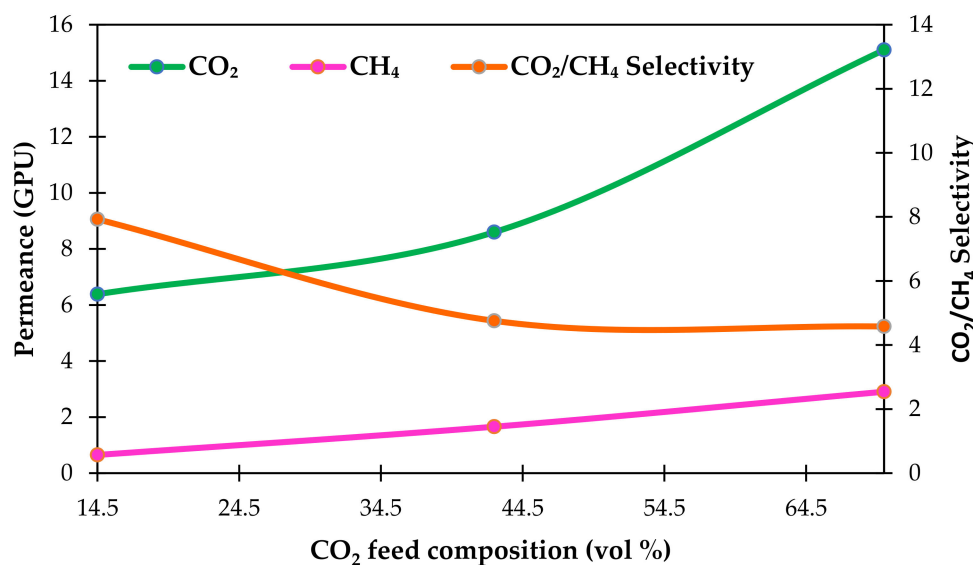


Figure 6. Effect of CO₂ feed concentration on CO₂ and CH₄ permeances and CO₂/CH₄ mixed gas selectivity in mixed gas separation at feed pressure of 5 bar.

As seen in Figure 6, CO₂ permeance steadily increases as CO₂ concentration increases, and vice versa for membrane selectivity. At a CO₂ feed concentration of 70 vol %, a maximum CO₂ permeance of 15.10 GPU is attained. Meanwhile, with a CO₂ feed concentration of 14.5 vol %, a minimum CO₂ permeance of 6.4 GPU is attained. Furthermore, under equal operating circumstances, the CO₂ permeance increase is modest for CO₂ concentrations below 40 vol %, being around 35%, compared to that for CO₂ concentrations beyond 40 vol %, which is about 76%.

However, the results demonstrate that selectivity declined as CO₂ feed concentration increased. The CO₂/CH₄ mixed gas selectivity showed a substantial decline from CO₂ feed concentrations of 14.5 vol % CO₂ to 70 vol % CO₂ (about 42%). Lower CO₂/CH₄ mixed gas selectivity was observed at higher CO₂ concentrations, despite the membrane showing larger CO₂ adsorption potential. This phenomenon is mainly due to the greater CH₄ adsorption capability of the membrane, which reduced the mixed gas selectivity [44]. As a result, a maximum CO₂/CH₄ mixed gas selectivity of 7.9 was obtained at a CO₂ feed concentration of 14.5 vol %. Furthermore, increasing the CO₂ feed concentration from 42.5 vol % to 70 vol % resulted in the saturation of the amine–CO₂ interaction, which aggregated CO₂ on the feed side of the membrane, thus lowering the CO₂/CH₄ mixed gas selectivity [46]. Additionally, a larger CO₂ feed concentration might inflate the polymer matrix, resulting in an increase in the rate of CH₄ penetration through the membrane [47].

From the results obtained in this work, we found that the selectivity of mixed gas is less than that of pure gases [48]. However, the mixed gas selectivity of CO₂/CH₄ is greater than the CO₂/CH₄ ideal selectivity at a CO₂ feed concentration of 14.5%, indicating that CO₂ and CH₄ compete for the adsorption site in the membrane. In comparison, at

a CO₂ feed concentration of 70 vol %, the CO₂ permeance rose by 112%, up to 15.1 GPU, compared to 7.1 GPU for pure gas permeation. Moreover, CO₂/CH₄ mixed gas selectivity reduced from 7.9 (CO₂ feed concentration of 14.5 vol %) to 4.6 (CO₂ feed concentration of 70 vol %), which is less than the CO₂/CH₄ ideal selectivity of 11.9 obtained in our previous work [25].

3.4.2. Effect of Feed Pressure

We further conducted the separation experiment on the C₁₀ membrane at different pressures up to 9 bar, and Figure 7 illustrates the effect of feed pressure from 1 to 9 bar on the performance of the C₁₀ membranes at 42.5 vol % CO₂ feed concentration.

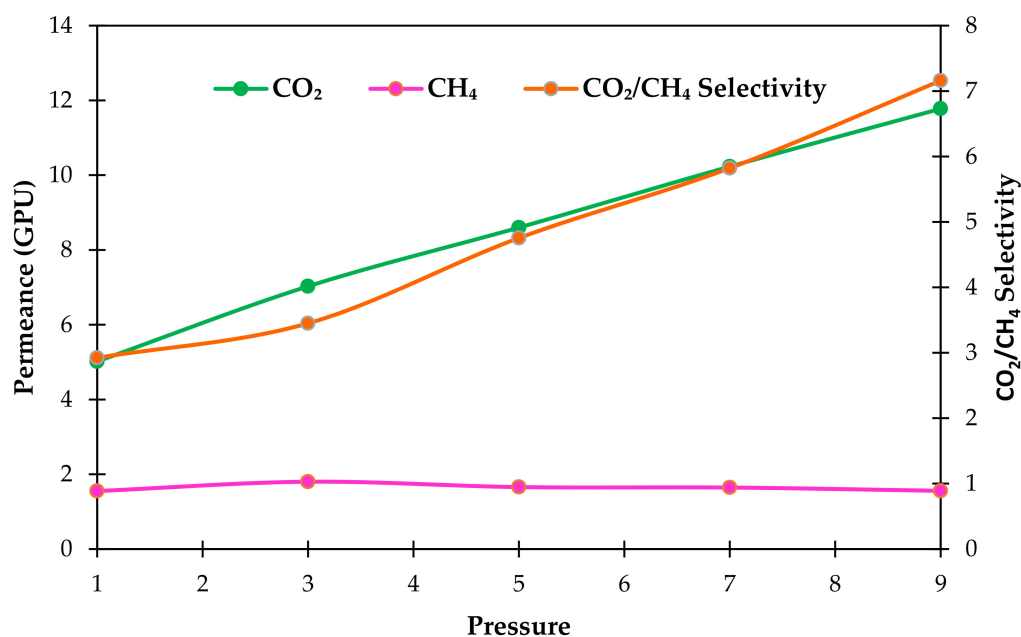


Figure 7. Effect of pressure on CO₂ and CH₄ permeances and CO₂/CH₄ mixed gas selectivity in mixed gas separation at 42.5 vol % CO₂ feed concentration.

Referring to Figure 7, increasing the feed pressure caused the increment of CO₂ and CH₄ permeance, as well as CO₂/CH₄ mixed gas selectivity. The maximum CO₂ permeance of 11.8 GPU was obtained at 9 bar. Meanwhile, at 1 bar, a minimum CO₂ permeance of 5.0 GPU was achieved. The CO₂ permeability rose 135%, from 5.0 GPU to 11.8 GPU, when the pressure was raised from 1 to 9 bar. However, a distinct pattern can be seen for the CH₄ permeability. It remained relatively consistent between 1.5 GPU and 1.8 GPU when the pressure increased from 1 to 9 bar. This phenomenon could be explained by greater CO₂ condensability as a result of its increased sorption capability.

Moreover, the increment of CO₂ permeance at higher pressures could be also related to the increase in gas solubility, caused by the enhancement of CO₂ molecule sorption in the polymeric network, where the CO₂ fills the gap between the polymer network's chains. This widens the distance between these bonds, and thus increases the mobility of the polymeric chain [46] and plasticizes the membrane. Eventually, the gas permeance and the gas compressibility of the membrane increase [49]. For all pressures investigated in this experiment, CO₂ permeance rose roughly linearly with increasing pressure, but CH₄ permeability decreased, showing competition for adsorption sites and, once again, preferential adsorption of CO₂ over CH₄ [50].

Furthermore, by increasing the feed pressure, CO₂/CH₄ mixed gas selectivity was also increased. When the pressure increased from 1 to 9 bar, the selectivity increased from 2.9 to 7.2 (Figure 7). This result is mainly due to higher CO₂ condensability compared to CH₄ (T_c of CO₂ is 31.1 °C compared to 82.3 °C for CH₄), which resulted in a stronger affinity of CO₂ to the membrane. Moreover, the kinetic diameter of CO₂ of 3.3 Å is smaller

than that of CH₄ (3.82 Å); therefore, the penetration rate of CO₂ over the membrane was greater than CH₄ [51]. In addition, the increase in mixed gas selectivity is also due to the inherent flexibility of NH₂-MIL-125(Ti) filler.

As can be seen from Figure 7, the CO₂ permeance and CO₂/CH₄ mixed gas selectivity of the membrane increase with increasing feed pressure. These results reveal that satisfactory separation performance can be maintained at higher pressure. Thus, it can be deduced that the PSF/PDMS/PEBAX/NH₂-MIL-125(Ti) membrane prepared in this work can be considered as a promising candidate for practical membrane-based natural gas purification.

4. Conclusions

Multilayer composite hollow fiber membranes containing NH₂-MIL-125(Ti) particles were fabricated using the dip-coating technique and assessed for CO₂/CH₄ separation at various CO₂ feed concentrations and feed pressures. Additionally, the chemical structure, phase structure, and morphology of the membrane were studied using different analytical tools. The XRD patterns showed the typical NH₂-MIL-125(Ti) structure peaks with an amorphous state in the membranes, and no crystallization of the NH₂-MIL-125(Ti) was found during the coating procedure in the composite membranes. FTIR results revealed that the addition of more particles into the polymer matrix resulted in no new peaks for all the composite membranes, implying the physical blending feature of NH₂-MIL-125(Ti) and within the PEBAX bulk. CO₂ permeance was greatest at a 70 vol % CO₂ feed composition, but it decreased slightly compared to single gas permeation. The highest CO₂/CH₄ mixed gas selectivity obtained was 7.9 at a CO₂ concentration of 14.5 vol % and testing pressure of 5 bar. The results of the mixed gas separation analysis indicate that the fabricated composite membrane can be considered as a viable alternative membrane material for gas separation processes.

Author Contributions: S.Z.: Formal analysis, investigation, data curation, writing—original draft, visualization. Y.F.Y.: Conceptualization, methodology, validation, resources, writing—review and editing, supervision, funding acquisition, project administration. N.J.: Conceptualization, methodology, resources, supervision. L.S.T.: Supervision. All authors have read and agreed to the published version of the manuscript.

Funding: This research was funded by Yayasan Universiti Teknologi PETRONAS] YUTP Grant (Cost Center: 015LC0-099).

Institutional Review Board Statement: Not applicable.

Informed Consent Statement: Not applicable.

Data Availability Statement: Not applicable.

Acknowledgments: The financial and technical supports provided by the Yayasan Universiti Teknologi PETRONAS (YUTP) Research Grant and the CO₂ Research Centre, Universiti Teknologi PETRONAS, are duly acknowledged.

Conflicts of Interest: The authors declare no conflict of interest.

References

1. Shah, M.S.; Tsapatsis, M.; Siepmann, J.I. Hydrogen Sulfide Capture: From Absorption in Polar Liquids to Oxide, Zeolite, and Metal–Organic Framework Adsorbents and Membranes. *Chem. Rev.* **2017**, *117*, 9755–9803. [[CrossRef](#)] [[PubMed](#)]
2. Mazyan, W.; Ahmadi, A.; Ahmed, H.; Hoorfar, M. Market and technology assessment of natural gas processing: A review. *J. Nat. Gas Sci. Eng.* **2016**, *30*, 487–514. [[CrossRef](#)]
3. Baker, R.W. and K.L. Natural Gas Processing with Membranes: An Overview. *Ind. Eng. Chem. Res.* **2008**, *47*, 2109–2121. [[CrossRef](#)]
4. Washim Uddin, M.; Hägg, M.-B. Natural gas sweetening—The effect on CO₂–CH₄ separation after exposing a facilitated transport membrane to hydrogen sulfide and higher hydrocarbons. *J. Membr. Sci.* **2012**, *423–424*, 143–149. [[CrossRef](#)]
5. Liu, G.; Chernikova, V.; Liu, Y.; Zhang, K.; Belmabkhout, Y.; Shekhah, O.; Zhang, C.; Yi, S.; Eddaoudi, M.; Koros, W.J. Mixed matrix formulations with MOF molecular sieving for key energy-intensive separations. *Nat. Mater.* **2018**, *17*, 283–289. [[CrossRef](#)]

6. Koronful, N.; Peters, K.; Ali, M.F.; Skulsangjuntr, J.; Jiang, L.; Kleine, A.; Basu, D.; Bencomo, J.; Hernandez, J.; Brink, G. Carbon Dioxide in Reservoir Gases: New Insights from Basin and Petroleum System Modeling. In *SPE Asia Pacific Oil and Gas Conference and Exhibition*; OnePetro: London, UK, 2018; Volume 1, p. 3121. [\[CrossRef\]](#)
7. Choi, Y.-S.; Nešić, S. Determining the corrosive potential of CO₂ transport pipeline in high pCO₂–water environments. *Int. J. Greenh. Gas Control* **2011**, *5*, 788–797. [\[CrossRef\]](#)
8. Zornoza, B.; Martinez-Joaristi, A.; Serra-Crespo, P.; Tellez, C.; Coronas, J.; Gascon, J.; Kapteijn, F. Functionalized flexible MOFs as fillers in mixed matrix membranes for highly selective separation of CO₂ from CH₄ at elevated pressures. *Chem. Commun.* **2011**, *47*, 9522–9524. [\[CrossRef\]](#)
9. Khan, I.U.; Othman, M.H.D.; Jilani, A.; Ismail, A.F.; Hashim, H.; Jaafar, J.; Zulhairun, A.K.; Rahman, M.A.; Rehman, G.U. ZIF-8 based polysulfone hollow fiber membranes for natural gas purification. *Polym. Test.* **2020**, *84*, 106415. [\[CrossRef\]](#)
10. Robeson, L.M. The upper bound revisited. *J. Membr. Sci.* **2008**, *320*, 390–400. [\[CrossRef\]](#)
11. Suleman, M.S.; Lau, K.K.; Yeong, Y.F. Development, characterization and performance evaluation of a swelling resistant membrane for CO₂/CH₄ separation. *J. Nat. Gas Sci. Eng.* **2018**, *52*, 390–400. [\[CrossRef\]](#)
12. Ismail, A.F.; Lorna, W. Suppression of plasticization in polysulfone membranes for gas separations by heat-treatment technique. *Sep. Purif. Technol.* **2003**, *30*, 37–46. [\[CrossRef\]](#)
13. Roslan, R.A.; Lau, W.J.; Sakthivel, D.B.; Khademi, S.; Zulhairun, A.K.; Goh, P.S.; Ismail, A.F.; Chong, K.C.; Lai, S.O. Separation of CO₂/CH₄ and O₂/N₂ by polysulfone hollow fiber membranes: Effects of membrane support properties and surface coating materials. *J. Polym. Eng.* **2018**, *38*, 871–880. [\[CrossRef\]](#)
14. Zulhairun, A.K.; Fachrurrazi, Z.G.; Nur Izwanne, M.; Ismail, A.F. Asymmetric hollow fiber membrane coated with polydimethylsiloxane–metal organic framework hybrid layer for gas separation. *Sep. Purif. Technol.* **2015**, *146*, 85–93. [\[CrossRef\]](#)
15. Li, T.; Pan, Y.; Peinemann, K.-V.; Lai, Z. Carbon dioxide selective mixed matrix composite membrane containing ZIF-7 nano-fillers. *J. Membr. Sci.* **2013**, *425–426*, 235–242. [\[CrossRef\]](#)
16. Lin, H.; Freeman, B.D. Materials selection guidelines for membranes that remove CO₂ from gas mixtures. *J. Mol. Struct.* **2005**, *739*, 57–74. [\[CrossRef\]](#)
17. Li, G.; Kujawski, W.; Válek, R.; Koter, S. A review-The development of hollow fibre membranes for gas separation processes. *Int. J. Greenh. Gas Control* **2021**, *104*, 103195. [\[CrossRef\]](#)
18. Chung, T.S. Calculation of the intrusion depth and its effects on microporous composite membranes. *Sep. Purif. Technol.* **1997**, *12*, 17–23. [\[CrossRef\]](#)
19. Yang, H.-C.; Hou, J.; Chen, V.; Xu, Z.-K. Surface and interface engineering for organic–inorganic composite membranes. *J. Mater. Chem. A* **2016**, *4*, 9716–9729. [\[CrossRef\]](#)
20. Chen, H.Z.; Thong, Z.; Li, P.; Chung, T.-S. High performance composite hollow fiber membranes for CO₂/H₂ and CO₂/N₂ separation. *Int. J. Hydrogen Energy* **2014**, *39*, 5043–5053. [\[CrossRef\]](#)
21. Liu, S.L.; Shao, L.; Chua, M.L.; Lau, C.H.; Wang, H.; Quan, S. Recent progress in the design of advanced PEO-containing membranes for CO₂ removal. *Prog. Polym. Sci.* **2013**, *38*, 1089–1120. [\[CrossRef\]](#)
22. Sutrisna, P.D.; Hou, J.; Li, H.; Zhang, Y.; Chen, V. Improved operational stability of Pebax-based gas separation membranes with ZIF-8: A comparative study of flat sheet and composite hollow fibre membranes. *J. Membr. Sci.* **2017**, *524*, 266–279. [\[CrossRef\]](#)
23. Suhaimi, N.H.; Yeong, Y.F.; Jusoh, N.; Chew, T.L.; Bustam, M.A.; Suleman, S. Separation of CO₂ from CH₄ using mixed matrix membranes incorporated with amine functionalized MIL-125 (Ti) nanofiller. *Chem. Eng. Res. Des.* **2020**, *159*, 236–247. [\[CrossRef\]](#)
24. Waqas Anjum, M.; Bueken, B.; De Vos, D.; Vankelecom, I.F.J. MIL-125(Ti) based mixed matrix membranes for CO₂ separation from CH₄ and N₂. *J. Membr. Sci.* **2016**, *502*, 21–28. [\[CrossRef\]](#)
25. Zakariya, S.; Yeong, Y.F.; Jusoh, N.; Tan, L.S. Fabrication of multilayer composite hollow fiber membrane comprising NH₂-MIL-125 (Ti) for CO₂ removal from CH₄. *Mater. Today Proc.* **2021**. Peerreview. [\[CrossRef\]](#)
26. Brunetti, A.; Tocci, E.; Cersosimo, M.; Kim, J.S.; Lee, W.H.; Seong, J.G.; Lee, Y.M.; Drioli, E.; Barbieri, G. Mutual influence of mixed-gas permeation in thermally rearranged poly(benzoxazole-co-imide) polymer membranes. *J. Membr. Sci.* **2019**, *580*, 202–213. [\[CrossRef\]](#)
27. Sánchez-Laínez, J.; Gracia-Guillén, I.; Zornoza, B.; Téllez, C.; Coronas, J. Thin supported MOF based mixed matrix membranes of Pebax[®] 1657 for biogas upgrade. *New J. Chem.* **2019**, *43*, 312–319. [\[CrossRef\]](#)
28. Sridhar, S.; Bee, S.; Bhargava, S. Membrane-based Gas Separation: Principle, Applications and Future Potential. *Chem. Eng. Dig.* **2014**, *2014*.
29. Mubashir, M.; Yeong, Y.F.; Chew, T.L.; Lau, K.K. Optimization of spinning parameters on the fabrication of NH₂-MIL-53(Al)/cellulose acetate (CA) hollow fiber mixed matrix membrane for CO₂ separation. *Sep. Purif. Technol.* **2019**, *215*, 32–43. [\[CrossRef\]](#)
30. Jusoh, N.; Lau, K.K.; Shariff, A.M.; Yeong, Y.F. Capture of bulk CO₂ from methane with the presence of heavy hydrocarbon using membrane process. *Int. J. Greenh. Gas Control* **2014**, *22*, 213–222. [\[CrossRef\]](#)
31. Genduso, G.; Wang, Y.; Ghanem, B.; Pinnau, I. Permeation, sorption, and diffusion of CO₂-CH₄ mixtures in polymers of intrinsic microporosity: The effect of intrachain rigidity on plasticization resistance. *J. Membr. Sci.* **2019**, *584*, 100–109. [\[CrossRef\]](#)
32. Jusoh, N.; Yeong, Y.F.; Lau, K.K.; Shariff, A.M. Fabrication of silanated zeolite T/6FDA-durene composite membranes for CO₂/CH₄ separation. *J. Clean. Prod.* **2017**, *166*, 1043–1058. [\[CrossRef\]](#)

33. Khanbabaee, G.; Aalaei, J.; Rahmatpour, A. Polymeric Nanocomposite Membranes for Gas Separation. *Sustain. Membr. Technol. Energy Water Environ.* **2012**, *87*–94. Available online: https://books.google.com.hk/books?hl=en&lr=&id=-56-IsIkeLsC&oi=fnd&pg=PA87&dq=Polymeric+Nanocomposite+Membranes+for+Gas+Separation.&ots=sKS8HMdjf2&sig=8pJtM5skDGgZlfEBDsAjqI8q3kl&redir_esc=y&hl=zh-CN&sourceid=cndr#v=onepage&q=Polymeric%20Nanocomposite%20Membranes%20for%20Gas%20Separation.&f=false (accessed on 10 February 2022).
34. Ghasemi Estahbanati, E.; Omidkhah, M.; Ebadi Amooghin, A. Interfacial Design of Ternary Mixed Matrix Membranes Containing Pebax 1657/Silver-Nanopowder/[BMIM][BF₄] for Improved CO₂ Separation Performance. *ACS Appl. Mater. Interfaces* **2017**, *9*, 10094–10105. [[CrossRef](#)]
35. Bharali, P.; Borthakur, S.; Hazarika, S. Selective Permeation of CO₂ through Amine Bearing Facilitated Transport Membranes. *J. Membr. Sci. Technol.* **2020**, *203*. [[CrossRef](#)]
36. Gong, X.-Y.; Huang, Z.-H.; Zhang, H.; Liu, W.-L.; Ma, X.-H.; Xu, Z.-L.; Tang, C.Y. Novel high-flux positively charged composite membrane incorporating titanium-based MOFs for heavy metal removal. *Chem. Eng. J.* **2020**, *398*, 125706. [[CrossRef](#)]
37. Zhu, X.; Yu, Z.; Liu, Y.; Li, X.; Long, R.; Wang, P.; Wang, J. NH₂-MIL-125@PAA composite membrane for separation of oil/water emulsions and dyes. *Colloids Surfaces A Physicochem. Eng. Asp.* **2021**, *630*, 127542. [[CrossRef](#)]
38. Wang, M.; Yang, L.; Yuan, J.; He, L.; Song, Y.; Zhang, H.; Zhang, Z.; Fang, S. Heterostructured Bi₂S₃@NH₂-MIL-125(Ti) nanocomposite as a bifunctional photocatalyst for Cr(vi) reduction and rhodamine B degradation under visible light. *RSC Adv.* **2018**, *8*, 12459–12470. [[CrossRef](#)]
39. Yin, S.; Chen, Y.; Li, M.; Hu, Q.; Ding, Y.; Shao, Y.; Di, J.; Xia, J.; Li, H. Construction of NH₂-MIL-125(Ti)/Bi₂WO₆ composites with accelerated charge separation for degradation of organic contaminants under visible light irradiation. *Green Energy Environ.* **2020**, *5*, 203–213. [[CrossRef](#)]
40. Yang, J.; Zhou, Q.; Shen, K.; Song, N.; Ni, L. Controlling nanodomain morphology of epoxy thermosets templated by poly(caprolactone)-block-poly(dimethylsiloxane)-block-poly(caprolactone) ABA triblock copolymer. *RSC Adv.* **2018**, *8*, 3705–3715. [[CrossRef](#)]
41. Yuan, F.; Wang, Z.; Li, S.; Wang, J.; Wang, S. Formation–structure–performance correlation of thin film composite membranes prepared by interfacial polymerization for gas separation. *J. Membr. Sci.* **2012**, *421–422*, 327–341. [[CrossRef](#)]
42. Shen, J.; Liu, G.; Huang, K.; Li, Q.; Guan, K.; Li, Y.; Jin, W. UiO-66-polyether block amide mixed matrix membranes for CO₂ separation. *J. Membr. Sci.* **2016**, *513*, 155–165. [[CrossRef](#)]
43. Sanaeepur, H.; Ahmadi, R.; Sinaei, M.; Kargari, A. Pebax-Modified Cellulose Acetate Membrane for CO₂/N₂ Separation. *J. Membr. Sci. Res.* **2019**, *5*, 25–32. [[CrossRef](#)]
44. Lee, M.-S.; Park, M.; Kim, H.; Park, S.-J. Effects of Microporosity and Surface Chemistry on Separation Performances of N-Containing Pitch-Based Activated Carbons for CO₂/N₂ Binary Mixture. *Sci. Rep.* **2016**, *6*, 23224. [[CrossRef](#)]
45. Halim, M.; Kadirkhan, F.; Mustapa, W.; Soh, W.K.; Yeo, S. Natural gas sweetening polymeric membrane: Established optimum operating condition at 70% of CO₂ concentration feed gas stream. *Malays. J. Fundam. Appl. Sci.* **2020**, *16*, 54–58. [[CrossRef](#)]
46. Ismail, A.F.; Yaacob, N. Performance of treated and untreated asymmetric polysulfone hollow fiber membrane in series and cascade module configurations for CO₂/CH₄ gas separation system. *J. Membr. Sci.* **2006**, *275*, 151–165. [[CrossRef](#)]
47. Falbo, F.; Brunetti, A.; Barbieri, G.; Drioli, E.; Tasselli, F. CO₂/CH₄ separation by means of Matrimid hollow fibre membranes. *Appl. Petrochem. Res.* **2016**, *6*, 439–450. [[CrossRef](#)]
48. Zhang, Y.; Musselman, I.H.; Ferraris, J.P.; Balkus, K.J. Gas permeability properties of Matrimid[®] membranes containing the metal-organic framework Cu-BPY-HFS. *J. Membr. Sci.* **2008**, *313*, 170–181. [[CrossRef](#)]
49. Li, X.; Jiang, Z.; Wu, Y.; Zhang, H.; Cheng, Y.; Guo, R.; Wu, H. High-performance composite membranes incorporated with carboxylic acid nanogels for CO₂ separation. *J. Membr. Sci.* **2015**, *495*, 72–80. [[CrossRef](#)]
50. Rios, R.; Stragliotto, F.; Peixoto, H.; Torres, A.; Bastos-Neto, M.; Azevedo, D.; Cavalcante, C., Jr. Studies on the adsorption behavior of CO₂-CH₄ mixtures using activated carbon. *Braz. J. Chem. Eng.* **2013**, *30*, 939–951. [[CrossRef](#)]
51. Wang, S.-E.; Huang, Y.; Hu, K.; Tian, J.; Zhao, S. A highly sensitive and selective aptasensor based on fluorescence polarization for the rapid determination of oncoprotein vascular endothelial growth factor (VEGF). *Anal. Methods* **2014**, *6*, 62–66. [[CrossRef](#)]